HHS Public Access

Author manuscript

Brain Stimul. Author manuscript; available in PMC 2022 August 16.

Published in final edited form as:

Brain Stimul. 2022 ; 15(4): 1002–1010. doi:10.1016/j.brs.2022.07.003.

Applications of open-source software ROAST in clinical studies: A review

Mohigul Nasimova[a], **Yu Huang**[a,b,*]

[a]Department of Biomedical Engineering, City College of the City University of New York, New York, NY, 10031, USA

[b]Department of Radiology, Memorial Sloan Kettering Cancer Center, New York, NY, 10065, USA

Abstract

Background: Transcranial electrical stimulation (TES) is broadly investigated as a therapeutic technique for a wide range of neurological disorders. The electric fields induced by TES in the brain can be estimated by computational models. A realistic and volumetric approach to simulate TES (ROAST) has been recently released as an open-source software package and has been widely used in TES research and its clinical applications. Rigor and reproducibility of TES studies have recently become a concern, especially in the context of computational modeling.

Methods: Here we reviewed 94 clinical TES studies that leveraged ROAST for computational modeling. When reviewing each study, we pay attention to details related to the rigor and reproducibility as defined by the locations of stimulation electrodes and the dose of stimulating current. Specifically, we compared across studies the electrode montages, stimulated brain areas, achieved electric field strength, and the relations between modeled electric field and clinical outcomes.

Results: We found that over 1800 individual heads have been modeled by ROAST for more than 30 different clinical applications. Similar electric field intensities were found to be reproducible by ROAST across different studies at the same brain area under same or similar stimulation montages.

Conclusion: This article reviews the use cases of ROAST and provides an overview of how ROAST has been leveraged to enhance the rigor and reproducibility of TES research and its applications.

1. Introduction

Transcranial electrical stimulation (TES) has been broadly investigated as a therapeutic technique for a wide range of neurological disorders such as major depression [1], epilepsy [2–5], Parkinson's disease [6], chronic pain [7,8], and stroke [9]. For more systematic

*Corresponding author. Department of Radiology, Memorial Sloan Kettering Cancer Center, New York, NY, 10065, USA. andypotatohy@gmail.com (Y. Huang).

Declaration of competing interest

We report no relevant conflicts of interest or industry support.

reviews, see Refs. [10,11]. The location of stimulation electrodes on the scalp and the exact dose of stimulating current contribute to the rigor and reproducibility of TES studies, as these factors directly determine the stimulation intensity and focality at the desired targets in the brain [12]. Computational models have been heavily used for estimating electric field distribution in each individual head [13–15]. However, these models are not readily accessible to medical doctors. Since the introduction of MRI-derived (i.e., individualized) models [13] and model validation [16], the use of current-flow models has greatly expanded to increase the study rigor (Fig. 1). However, proprietary engineering modeling tools (e.g., COMSOL, Abaqus) are technically sophisticated and difficult to implement for most medical doctors [13–15,17]. Open-source software usually have a steep learning curve for researchers without a solid background in computer science (e.g., SciRun, [18]. We recently released a realistic and volumetric approach to simulate TES (ROAST) which succeeds in terms of automation, ease-of-use, speed, and experimental validation [19]. Compared to the other major open-source software in the field, SimNIBS [15,20], ROAST advocates volumetric and realistic modeling of the anatomy in the head tissues and performed on par with SimNIBS when tested out-of-box on validation data [19,21].

As a new software in the field of TES research, ROAST has gained hundreds of users in a short period of time (Fig. 2). It has been used to model over 1800 individual heads spanning across 12 applications (Table 1). By ensuring the accuracy and replicability throughout the entire modeling process including head segmentation, electrode location and placement, and dose of the stimulation, ROAST helped enhance the rigor and reproducibility of TES studies. Various montages were modeled and electric field magnitudes at the same brain areas under similar montages were reproducible across different studies (Table 2). This paper reviews the adoptions of this software and the use cases in detail, in the hope that future TES research and applications can have a reference on how to leverage readily available computational models to enhance rigor and reproducibility.

2. Methods

2.1. Literature search

To find out the trend in the literature that utilized modeling for TES research, keywords “computational models transcranial electrical stimulation” were used to search the literature on PubMed. Number of publications by year was returned and plotted.

2.2. Adoptions of ROAST

Shortly after the release of ROAST, we have been tracking user downloads on the website that hosts ROAST (https://www.parralab.org/roast/) by Google Analytics. Daily downloads and geographic locations were stored and plotted.

2.3. Citation report

All the papers found on Google Scholar that cited ROAST publications [19,58] were reviewed in April 2022. For each paper, we looked up the number of subjects that were modeled by ROAST, the clinical applications of the subjects that were studied, and the purpose of computational modeling in that study.

2.4. Rigor and reproducibility

A workshop organized by the National Institute of Mental Health in 2016 discussed major factors contributing to the rigor and reproducibility of TES research [12]. The factors that relate to computational modeling include locations of the placed electrodes on the scalp and the dosing of the stimulation. To show how ROAST helps to enhance rigor and reproducibility in those clinical studies found on Google Scholar that used ROAST for modeling more than one individual head, we extracted the following information and compared them across studies: electrode montage and electrode type (conventional (C) vs. high-definition (HD)), stimulated brain areas, achieved intensity of electric field at the stimulated areas (normalized to 1 mA dose), correlation between modeled electric field and clinical outcomes, and subject characteristics (patients vs. healthy).

3. Results

3.1. Computational models of TES tend to be widely adopted

It is obvious that more and more TES studies start to use computational models (Fig. 1), especially since the introduction of individualized modeling from MRIs [13]. SimNIBS, SciRun, and ROAST all helped push the adoption of current-flow models in the literature. Specifically, ROAST has been downloaded 1598 times (1414 unique downloads; see Fig. 2) by April 2022.

3.2. ROAST has been heavily used for individualized TES modeling

According to Google Scholar, the papers in which ROAST was published [19,58] had been cited 225 times by April 2022. Among these, 15 are dissertations and 24 are reviews and book chapters. We reviewed the remaining 186 papers, and found 94 clinical TES studies that used ROAST for computational modeling. Table 1 summarizes all the results for each specific clinical application. As a reference, note that SimNIBS [15,20] has been cited over 800 times, and SciRun for TES simulation [18] has been cited 57 times. One of the studies in Table 1 also used SimNIBS to model the 32 heads but did not find any significant difference in predicted electric field compared to ROAST [45].

It is clear from Table 1 that ROAST has been applied in clinical studies spanning across 12 applications and modeled 1858 individual heads, thanks to its scripting feature that allows easy batch processing. Most of these studies used ROAST to visualize the stimulation electrodes and the electric field distribution at the region of interests (ROI), and to correlate the simulated electric field intensities at the ROIs with clinical outcomes. Some of these studies used ROAST to calculate the dosing of stimulation, optimize the stimulation montage, or perform voxel-based morphometry using the generated tissue segmentation. The study that modeled the most subjects was [22]; where N = 587 healthy older adults under TES were modeled. The results showed that the amount of stimulation current that reaches the brain decreases with increasing atrophy, suggesting that adjusting current dose in older adults based on degree of atrophy may be necessary to achieve desired stimulation benefits. It was not possible to perform TES modeling studies with rigor and reproducibility for over 500 subjects before ROAST was created, as one had to run head segmentation, electrode placement, and electric field computation by hand in various software [13,17,59],

where uncertainties may be introduced by manual operations of these software in the modeling process. Other representative studies include: Ref. [26] simulated N = 60 dementia patients to correlate the model-predicted electric field at ROIs with clinical data to evaluate the therapeutic efficacy of a multi-day TES regime on language impairment in patients with semantic dementia. Ref. [29] used ROAST to model N = 8 glioma patients in their study of TES feasibility on these patients. They showed that patient-specific modeling of electric field in the presence of tumor may contribute to understanding the dose-response relationship of this intervention. Ref. [32] modeled N = 18 subjects at different ages for cerebellar transcranial direct current stimulation and found that cerebellar shrinkage and increasing thickness of the highly conductive CSF during healthy aging can lead to the dispersion of the current away from the lobules underlying the active electrode. Ref. [36] built individualized models for N = 16 subjects to help determine the best montage for selective modulation of dorsal and ventral pathways of reading in bilinguals. Ref. [37] used ROAST to calculate the electric field intensities in N = 151 patients with severe depression undergoing electroconvulsive therapy (ECT) and found that the electric fields predicted by ROAST positively correlate with the volumetric changes of the brain due to ECT. Ref. [39] compared *in vivo* measured electric fields during TES on N = 12 epilepsy patients with their individual models generated by ROAST to validate the models. Ref. [40] built N = 10 individualized models using ROAST to study if electric field intensities at the ROIs positively correlate with functional connectivity. Another relatively large study [48] leveraged ROAST to model N = 240 individuals to study the effects of cortical anatomical parameters such as volumes, dimension, and torque on simulated TES current density in healthy young, middle-aged, and older males and females. Ref. [53] modeled N = 21 individual heads to assess the target engagement in their study of TES on antipsychotic-resistant auditory verbal hallucinations in schizophrenia. Refs. [55,56] built individualized head models for N = 5 subjects to compute the optimal electrode montage to target the cortico-cerebello-thalamo-cortical loop for improving substance use disorder. Ref. [57] modeled N = 15 subjects to predict significant changes of functional connectivity observed in the working memory network from an acute TES application.

In addition, many studies run the models on the example head included with ROAST or an individual sample from the investigators. These work cover various clinical applications including: attention-deficit hyperactivity disorder [61,62], aging [63], associative memory [64,65], attention [66–68], body awareness [69], cognitive control and function [70]; Fusco et al. [125]; [71,72], connectivity [73], decision making [74–77]; Schulreich and Schwabe [126], declarative learning [78], depressive disorder [79], electroencephalography (EEG) research [80–83], imitation [84], memory retrieval [85–87], mind wandering [88,89], motor learning [90–95], motor skills [96–98], neurorehabilitation [60], neurovascular coupling [99], obsessive-compulsive disorder [100], phantom limb pain [101], post-anoxic leukoencephalopathy [102], reading speed [103], schizophrenia [104], social anxiety disorder [105], stroke [106], visual perception [107,108], and working memory [109–115].

Note that for those studies that involved subjects with pathological head anatomies (e.g., tumor or lesion), customized segmentation was performed and integrated into the ROAST pipeline to account for these anatomies [25,29]. This is because the segmentation function in ROAST [116] was developed for normal head anatomy only.

3.3. ROAST helps to enhance the rigor and reproducibility

From Table 2, we can see that ROAST has been used to model various electrode montages to stimulate different brain areas. 29 out of the 35 studies in Table 2 used bipolar montages, and 21 of these bipolar montages are conventional pad electrodes. Most of the studies in Table 2 were interested in stimulating the primary motor cortex (M1), frontal cortex and cerebellum. For the primary motor cortex, Ref. [29] used bipolar montage C3-FP1 with conventional electrodes and achieved an average electric field of 0.12 V/m at the left M1 with 1 mA stimulating current. Ref. [42] obtained an average of 0.19 V/m under montage CP5-FC1 with high-definition electrodes, and 0.18 V/m under montage C3-FP2. Ref. [44] achieved 0.16 V/m averaged electric field with high-definition electrodes Fp2-CCP3. For the frontal cortex, Ref. [25] obtained a peak electric field of 0.3 V/m with montage F3–F4 using conventional electrodes. With the same montage, Ref. [46] achieved a median electric field of 0.047 V/m at inferior frontal gyrus. Also with the same montage but high-definition electrodes, Ref. [47] showed an electric field in the range of 0.06–0.10 V/m in the frontal cortex. With montage F3 and the right supraorbital, Ref. [52] outputs an average current density of 0.12 mA/m^2 at the left middle frontal gyrus. For the cerebellum, both [33,34] report an average of about 0.05 V/m under the same montage of PO9h–PO10h using high-definition electrodes. These results suggest that ROAST may help to enhance the rigor of TES models as similar electric field intensities were reproducible across different studies at the same brain area under same or similar stimulation montages.

In Table 2, 21 out of the 35 studies focus on healthy subjects including old and young adults. The other 14 studies in Table 2 build models for patients with the corresponding clinical applications in Table 1. For all the studies in Table 1 with Use Purpose (I), i.e., ROI analysis of E-field against clinical outcomes, we noted in Table 2 the detailed correlation between the predicted electric field and the studied clinical outcome/metric. Except one study [46], all the other studies in Table 2 report significant correlations between the electric field intensity and the outcome of stimulation or the inter-individual variability.

4. Discussions and conclusions

It is clear that computational models are becoming more and more intensively used in the research and clinical applications of TES to enhance rigor and reproducibility. As a new modeling tool in the TES community, ROAST can be improved in several ways to further strengthen study rigor and reproducibility: (1) ROI analysis: a function that allows users to automatically read out electric fields at the ROIs either in the individual head or the standard head space [117]. (2) Interface with other open-source software. For example, researchers in source imaging using electroencephalography/magnetoencephalography (EEG/MEG) rely on the same forward models that ROAST generates [118]. We have developed an interface [119] that allows users to import the models of a standard head from ROAST into Brainstorm, a popular software for EEG/MEG source localization [120]. (3) Interface of customized segmentation. This will allow users to add additional, customized geometry in the model. (4) Integration of modern deep-learning engine for segmentation of pathological head anatomies mostly presented in clinical populations [121]. This will significantly expand the clinical adoptions of this software, as the conventional segmentation algorithm

used by ROAST [116] is not capable of handling pathological heads. (5) Development of a platform that allows calibration of tissue conductivities for more accurate and personalized modeling. TES models overestimate the electric field compared to intracranial electrical recordings [16], but underestimate the magnetic field induced by the stimulation current compared to actual measurements [122]. Future work will leverage state-of-the-art recording techniques such as in-vivo stereotactic EEG electrodes inserted into the deep brain [123], or in-vivo imaging of magnetic fields in the head induced by the stimulation current [124] to calibrate the models and derive individualized tissue conductivities. This will facilitate more precise dosing and spatial targeting for the stimulation.

In conclusion, the era of precise medicine has come including clinical applications of TES where highly individualized and accurate computational models are becoming more readily accessible with constantly improved software and computational power.

Acknowledgements

This work was supported by the National Institutes of Health through grants P30CA008748 and R01CA247910. Support was also provided by the Memorial Sloan Kettering Cancer Center Department of Radiology.

References

[1]. Bikson M, Bulow P, Stiller J, Datta A, Battaglia F, Karnup S, Postolache T. Transcranial direct current stimulation for major depression: a general system for quantifying transcranial electrotherapy dosage. Curr Treat Options Neurol 2008;10:377–85. 10.1007/s11940-008-0040-y. [PubMed: 18782510]

[2]. Auvichayapat N, Rotenberg A, Gersner R, Ngodklang S, Tiamkao S, Tassaneeyakul W, Auvichayapat P. Transcranial direct current stimulation for treatment of refractory childhood focal epilepsy. Brain Stimul 2013;6: 696–700. 10.1016/j.brs.2013.01.009. [PubMed: 23415937]

[3]. Fregni F, Thome-Souza S, Nitsche MA, Freedman SD, Valente KD, Pascual-Leone A. A controlled clinical trial of cathodal DC polarization in patients with refractory epilepsy. Epilepsia 2006b;47:335–42. 10.1111/j.1528-1167.2006.00426.x. [PubMed: 16499758]

[4]. Regner GG, Pereira P, Leffa DT, de Oliveira C, Vercelino R, Fregni F, Torres ILS. Preclinical to clinical translation of studies of transcranial direct-current stimulation in the treatment of epilepsy: a systematic review. Front Neurosci 2018;12:189. 10.3389/fnins.2018.00189. [PubMed: 29623027]

[5]. San-Juan D, Morales-Quezada L, Orozco Garduoño AJ, Alonso-Vanegas M, González-Aragón MF, Espinoza López DA, Vázquez Gregorio R, Anschel DJ, Fregni F. Transcranial direct current stimulation in epilepsy. Brain Stimul 2015;8:455–64. 10.1016/j.brs.2015.01.001. [PubMed: 25697590]

[6]. Fregni F, Boggio PS, Santos MC, Lima M, Vieira AL, Rigonatti SP, Silva MTA, Barbosa ER, Nitsche MA, Pascual-Leone A. Noninvasive cortical stimulation with transcranial direct current stimulation in Parkinson's disease. Mov Disord 2006a;21:1693–702. 10.1002/mds.21012. [PubMed: 16817194]

[7]. Fregni F, Freedman S, Pascual-Leone A. Recent advances in the treatment of chronic pain with non-invasive brain stimulation techniques. Lancet Neurol 2007;6:188–91. 10.1016/S1474-4422(07)70032-7. [PubMed: 17239806]

[8]. Lefaucheur J-P. Cortical neurostimulation for neuropathic pain: state of the art and perspectives. Pain 2016;157(1). 10.1097/j.pain.0000000000000401. S81–S89. [PubMed: 26785160]

[9]. Meinzer M, Darkow R, Lindenberg R, Flöel A. Electrical stimulation of the motor cortex enhances treatment outcome in post-stroke aphasia. Brain 2016;139:1152–63. 10.1093/brain/aww002. [PubMed: 26912641]

[10]. Fregni F, El-Hagrassy MM, Pacheco-Barrios K, Carvalho S, Leite J, Simis M, Brunelin J, Nakamura-Palacios EM, Marangolo P, Venkatasubramanian G, San-Juan D, Caumo W, Bikson M, Brunoni AR, Neuromodulation Center Working Group. Evidence-based guidelines and secondary meta-analysis for the use of transcranial direct current stimulation in neurological and psychiatric disorders. Int J Neuropsychopharmacol 2021;24:256–313. 10.1093/ijnp/pyaa051. [PubMed: 32710772]

[11]. Lefaucheur J-P, Antal A, Ayache SS, Benninger DH, Brunelin J, Cogiamanian F, Cotelli M, De Ridder D, Ferrucci R, Langguth B, Marangolo P, Mylius V, Nitsche MA, Padberg F, Palm U, Poulet E, Priori A, Rossi S, Schecklmann M, Vanneste S, Ziemann U, Garcia-Larrea L, Paulus W. Evidence-based guidelines on the therapeutic use of transcranial direct current stimulation (tDCS). Clin Neurophysiol 2017;128:56–92. 10.1016/j.clinph.2016.10.087. [PubMed: 27866120]

[12]. Bikson M, Brunoni AR, Charvet LE, Clark VP, Cohen LG, Deng Z-D, Dmochowski J, Edwards DJ, Frohlich F, Kappenman ES, Lim KO, Loo C, Mantovani A, McMullen DP, Parra LC, Pearson M, Richardson JD, Rumsey JM, Sehatpour P, Sommers D, Unal G, Wassermann EM, Woods AJ, Lisanby SH. Rigor and reproducibility in research with transcranial electrical stimulation: an NIMH-sponsored workshop. Brain Stimul 2018;11:465–80. 10.1016/j.brs.2017.12.008. [PubMed: 29398575]

[13]. Datta A, Bansal V, Diaz J, Patel J, Reato D, Bikson M. Gyri eprecise head model of transcranial DC stimulation: improved spatial focality using a ring electrode versus conventional rectangular pad. Brain Stimul 2009;2:201–7. 10.1016/j.brs.2009.03.005. [PubMed: 20648973]

[14]. Ruffini G, Wendling F, Merlet I, Molaee-Ardekani B, Mekonnen A, Salvador R, Soria-Frisch A, Grau C, Dunne S, Miranda PC. Transcranial current brain stimulation (tCS): models and technologies. IEEE Trans Neural Syst Rehabil Eng 2013;21:333–45. 10.1109/TNSRE.2012.2200046. [PubMed: 22949089]

[15]. Windhoff M, Opitz A, Thielscher A. Electric field calculations in brain stimulation based on finite elements: an optimized processing pipeline for the generation and usage of accurate individual head models. Hum Brain Mapp 2011. 10.1002/hbm.21479. n/a-n/a.

[16]. Huang Y, Liu AA, Lafon B, Friedman D, Dayan M, Wang X, Bikson M, Doyle WK, Devinsky O, Parra LC. Measurements and models of electric fields in the in vivo human brain during transcranial electric stimulation. eLife 2017;6:e18834. 10.7554/eLife.18834. [PubMed: 28169833]

[17]. Huang Y, Dmochowski JP, Su Y, Datta A, Rorden C, Parra LC. Automated MRI segmentation for individualized modeling of current flow in the human head. J Neural Eng 2013;10:066004. 10.1088/1741-2560/10/6/066004. [PubMed: 24099977]

[18]. Dannhauer M, Brooks D, Tucker D, MacLeod R. A pipeline for the simulation of transcranial direct current stimulation for realistic human head models using SCIRun/BioMesh3D. In: 2012 annual international conference of the IEEE engineering in medicine and biology society (EMBC). Presented at the 2012 annual international conference of the IEEE engineering in medicine and biology society. EMBC; 2012. p. 5486–9. 10.1109/EMBC.2012.6347236.

[19]. Huang Y, Datta A, Bikson M, Parra LC. Realistic volumetric-approach to simulate transcranial electric stimulationd–ROAST–a fully automated open-source pipeline. J Neural Eng 2019;16:056006. 10.1088/1741-2552/ab208d. [PubMed: 31071686]

[20]. Thielscher A, Antunes A, Saturnino GB. Field modeling for transcranial magnetic stimulation: a useful tool to understand the physiological effects of TMS?. In: 2015 37th annual international conference of the IEEE engineering in medicine and biology society (EMBC). Presented at the 2015 37th annual international conference of the IEEE engineering in medicine and biology society. EMBC; 2015. p. 222–5. 10.1109/EMBC.2015.7318340.

[21]. Puonti O, Saturnino GB, Madsen KH, Thielscher A. Value and limitations of intracranial recordings for validating electric field modeling for transcranial brain stimulation. Neuroimage 2020;208:116431. 10.1016/j.neuroimage.2019.116431. [PubMed: 31816421]

[22]. Indahlastari A, Albizu A, O'Shea A, Forbes MA, Nissim NR, Kraft JN, Evangelista ND, Hausman HK, Woods AJ. Modeling transcranial electrical stimulation in the aging brain. Brain Stimul 2020;13:664–74. 10.1016/j.brs.2020.02.007. [PubMed: 32289695]

[23]. Indahlastari A, Albizu A, Boutzoukas EM, O'Shea A, Woods AJ. White matter hyperintensities affect transcranial electrical stimulation in the aging brain. Brain Stimul 2021a;14:69–73. 10.1016/j.brs.2020.11.009. [PubMed: 33217610]

[24]. Lu H, Li J, Zhang L, Chan SSM, Lam LCW, for the Open Access Series of Imaging Studies. Dynamic changes of region-specific cortical features and scalp-to-cortex distance: implications for transcranial current stimulation modeling. J NeuroEng Rehabil 2021;18:2. 10.1186/s12984-020-00764-5. [PubMed: 33397402]

[25]. Im JJ, Jeong H, Bikson M, Woods AJ, Unal G, Oh JK, Na S, Park J-S, Knotkova H, Song I-U, Chung Y-A. Effects of 6-month at-home transcranial direct current stimulation on cognition and cerebral glucose metabolism in Alzheimer's disease. Brain Stimul 2019;12:1222–8. 10.1016/j.brs.2019.06.003. [PubMed: 31196835]

[26]. Sanches C, Levy R, Benisty S, Volpe-Gillot L, Habert M-O, Kas A, Ströer S, Pyatigorskaya N, Kaglik A, ourbon A, Dubois B, Migliaccio R, Valero-Cabré A, Teichmann M. Testing the therapeutic effects of transcranial direct current stimulation (tDCS) in semantic dementia: a double blind, sham controlled, randomized clinical trial. Trials 2019;20:632. 10.1186/s13063-019-3613-z. [PubMed: 31747967]

[27]. Lang ST, Gan LS, McLennan C, Monchi O, Kelly JJP. Impact of peritumoral edema during tumor treatment field therapy: a computational modelling study. IEEE (Inst Electr Electron Eng) Trans Biomed Eng 2020b;67:3327–38. 10.1109/TBME.2020.2983653.

[28]. Arora Y, Chowdhury SR. Cortical excitability through anodal transcranial direct current stimulation: a computational approach. J Med Syst 2020;44:48. 10.1007/s10916-019-1490-3. [PubMed: 31900599]

[29]. Lang S, Gan LS, McLennan C, Kirton A, Monchi O, Kelly JJP. Preoperative transcranial direct current stimulation in glioma patients: a proof of concept pilot study. Front Neurol 2020a;11.

[30]. Zhang X, Hancock R, Santaniello S. Transcranial direct current stimulation of cerebellum alters spiking precision in cerebellar cortex: a modeling study of cellular responses. PLoS Comput Biol 2021;17:e1009609. 10.1371/journal.pcbi.1009609. [PubMed: 34882680]

[31]. Rezaee Z, Ranjan S, Solanki D, Bhattacharya M, Srivastava MVP, Lahiri U, Dutta A. Feasibility of combining functional near-infrared spectroscopy with electroencephalography to identify chronic stroke responders to cerebellar transcranial direct current stimulation—a computational modeling and portable neuroimaging methodological study. Cerebellum 2021;20:853–71. 10.1007/s12311-021-01249-4. [PubMed: 33675516]

[32]. Rezaee Z, Dutta A. Lobule-specific dosage considerations for cerebellar transcranial direct current stimulation during healthy aging: a computational modeling study using age-specific magnetic resonance imaging templates. Neuromodulation: Technology at the Neural Interface 2020;23: 341–65. 10.1111/ner.13098. [PubMed: 31995268]

[33]. Rezaee Z, Kaura S, Solanki D, Dash A, Srivastava MVP, Lahiri U, Dutta A. Deep cerebellar transcranial direct current stimulation of the dentate nucleus to facilitate standing balance in chronic stroke survivors—a pilot study. Brain Sci 2020;10:94. 10.3390/brainsci10020094.

[34]. Solanki D, Rezaee Z, Dutta A, Lahiri U. Investigating the feasibility of cerebellar transcranial direct current stimulation to facilitate post-stroke over-ground gait performance in chronic stroke: a partial least-squares regression approach. J NeuroEng Rehabil 2021;18:18. 10.1186/s12984-021-00817-3. [PubMed: 33509192]

[35]. Moussa-Tooks AB, Cheng H, Burroughs LP, Rejimon AC, Hetrick WP. Cerebellar tDCS consistency and metabolite changes: a recommendation to decrease barriers to replicability. Brain Stimul: Basic, Translational, and Clinical Research in Neuromodulation 2020. 10.1016/j.brs.2020.08.005.0.

[36]. Bhattacharjee S, Kashyap R, O'Brien BA, McCloskey M, Oishi K, Desmond JE, Rapp B, Chen SHA. Reading proficiency influences the effects of transcranial direct current stimulation: evidence from selective modulation of dorsal and ventral pathways of reading in bilinguals. Brain Lang 2020;210:104850. 10.1016/j.bandl.2020.104850. [PubMed: 32890855]

[37]. Argyelan M, Oltedal L, Deng Z-D, Wade B, Bikson M, Joanlanne A, Sanghani S, Bartsch H, Cano M, Dale AM, Dannlowski U, Dols A, Enneking V, Espinoza R, Kessler U, Narr KL, Oedegaard KJ, Oudega ML, Redlich R, Stek ML, Takamiya A, Emsell L, Bouckaert F, Sienaert P, Pujol J, Tendolkar I, van Eijndhoven P, Petrides G, Malhotra AK, Abbott C. Electric

field causes volumetric changes in the human brain. eLife 2019;8:e49115. 10.7554/eLife.49115. [PubMed: 31644424]

[38]. Wang M, Zhu S, Guan H, Jiang H, Zhang J, Zhang S. In: Vivo measurements of cranial electrical stimulation using stereotactic-EEG: a pilot study; 2021.p. 560–3. 10.1109/NER49283.2021.9441106.

[39]. Wang M, Han J, Jiang H, Zhu J, Feng W, Chhatbar PY, Zhang J, Zhang S. Intracranial electric field recording during multichannel transcranial electrical stimulation. 10.1101/2021.12.19.473336; 2021a.

[40]. Kar K, Ito T, Cole MW, Krekelberg B. Transcranial alternating current stimulation attenuates BOLD adaptation and increases functional connectivity. J Neurophysiol 2020;123:428–38. 10.1152/jn.00376.2019. [PubMed: 31825706]

[41]. Kasten FH, Duecker K, Maack MC, Meiser A, Herrmann CS. Integrating electric field modeling and neuroimaging to explain inter-individual variability of tACS effects. Nat Commun 2019;10:5427. 10.1038/s41467-019-13417-6. [PubMed: 31780668]

[42]. Evans C, Bachmann C, Lee JSA, Gregoriou E, Ward N, Bestmann S. Dose-controlled tDCS reduces electric field intensity variability at a cortical target site. Brain Stimul 2020;13:125–36. 10.1016/j.brs.2019.10.004. [PubMed: 31653475]

[43]. Albizu A, Fang R, Indahlastari A, O'Shea A, Stolte SE, See KB, Boutzoukas EM, Kraft JN, Nissim NR, Woods AJ. Machine learning and individual variability in electric field characteristics predict tDCS treatment response. Brain Stimul 2020;13:1753–64. 10.1016/j.brs.2020.10.001. [PubMed: 33049412]

[44]. Johnstone A, Zich C, Evans C, Lee J, Ward N, Bestmann S. The impact of brain lesions on tDCS-induced electric field magnitud. 10.1101/2021.03.19.436124; 2021.

[45]. Bhalerao GV, Sreeraj VS, Bose A, Narayanaswamy JC, Venkatasubramanian G. Comparison of electric field modeling pipelines for transcranial direct current stimulation. Neurophysiol Clin 2021;51:303–18. 10.1016/j.neucli.2021.05.002. [PubMed: 34023189]

[46]. Filmer HL, Ballard T, Ehrhardt SE, Bollmann S, Shaw TB, Mattingley JB, Dux PE. Dissociable effects of tDCS polarity on latent decision processes are associated with individual differences in neurochemical concentrations and cortical morphology. Neuropsychologia 2020;141:107433. 10.1016/j.neuropsychologia.2020.107433. [PubMed: 32184100]

[47]. Zanto TP, Jones KT, Ostrand AE, Hsu W-Y, Campusano R, Gazzaley A. Individual differences in neuroanatomy and neurophysiology predict effects of transcranial alternating current stimulation. Brain Stimul 2021;14:1317–29. 10.1016/j.brs.2021.08.017. [PubMed: 34481095]

[48]. Bhattacharjee S, Kashyap R, Goodwill AM, O'Brien BA, Rapp B, Oishi K, Desmond JE, Chen SHA. Sex difference in tDCS current mediated by changes in cortical anatomy: a study across young, middle and older adults. Brain Stimul 2022;15:125–40. 10.1016/j.brs.2021.11.018. [PubMed: 34826627]

[49]. Caulfield KA, Badran BW, DeVries WH, Summers PM, Kofmehl E, Li X, Borckardt JJ, Bikson M, George MS. Transcranial electrical stimulation motor threshold can estimate individualized tDCS dosage from reverse-calculation electric-field modeling. Brain Stimul 2020;13:961–9. 10.1016/j.brs.2020.04.007. [PubMed: 32330607]

[50]. Filmer HL, Ehrhardt SE, Shaw TB, Mattingley JB, Dux PE. The efficacy of transcranial direct current stimulation to prefrontal areas is related to underlying cortical morphology. Neuroimage 2019a;196:41–8. 10.1016/j.neuroimage.2019.04.026. [PubMed: 30978491]

[51]. Kashyap R, Bhattacharjee S, Arumugam R, Oishi K, Desmond JE, Chen SA. i-SATA: a MATLAB based toolbox to estimate current density generated by transcranial direct current stimulation in an individual brain. J Neural Eng 2020;17:056034. 10.1088/1741-2552/aba6dc. [PubMed: 32674087]

[52]. Kashyap R, Bhattacharjee S, Arumugam R, Bharath RD, Udupa K, Oishi K, Desmond JE, Chen SHA, Guan C. Focality-oriented selection of current dose for transcranial direct current stimulation. J Personalized Med 2021;11:940. 10.3390/jpm11090940.

[53]. Kantrowitz JT, Sehatpour P, Avissar M, Horga G, Gwak A, Hoptman MJ, Beggel O, Girgis RR, Vail B, Silipo G, Carlson M, Javitt DC. Significant improvement in treatment resistant auditory verbal hallucinations after 5 days of double-blind, randomized, sham controlled, fronto-

temporal, transcranial direct current stimulation (tDCS): a replication/extension study. Brain Stimul 2019;12:981–91. 10.1016/j.brs.2019.03.003. [PubMed: 30922713]

[54]. Mondino M, Fonteneau C, Simon L, Dondé C, Haesebaert F, Poulet E, Brunelin J. Advancing clinical response characterization to frontotemporal transcranial direct current stimulation with electric field distribution in patients with schizophrenia and auditory hallucinations: a pilot study. Eur Arch Psychiatr Clin Neurosci 2020. 10.1007/s00406-020-01149-4.

[55]. Dutta A, Ghosh A, Singh S. Deep cerebellar transcranial electrical stimulation: hypothesis and theory for cannabis use disorder. 10.20944/preprints202012.0178.v1; 2020.

[56]. Walia P, Ghosh A, Singh S, Dutta A. Portable neuroimaging-guided noninvasive brain stimulation of the cortico-cerebello-thalamo-cortical loop—hypothesis and theory in cannabis use disorder. Brain Sci 2022;12:445. 10.3390/brainsci12040445. [PubMed: 35447977]

[57]. Indahlastari A, Albizu A, Kraft JN, O'Shea A, Nissim NR, Dunn AL, Carballo D, Gordon MP, Taank S, Kahn AT, Hernandez C, Zucker WM, Woods AJ. Individualized tDCS modeling predicts functional connectivity changes within the working memory network in older adults. Brain Stimul: Basic, Translational, and Clinical Research in Neuromodulation 2021b;14:1205–15. 10.1016/j.brs.2021.08.003.

[58]. Huang Y, Datta A, Bikson M, Parra LC. ROAST: an open-source, fully-automated, realistic volumetric-approach-based simulator for TES. In: 2018 40th annual international conference of the IEEE engineering in medicine and biology society (EMBC). Presented at the 2018 40th annual international conference of the IEEE engineering in medicine and biology society. EMBC; 2018. p. 3072–5. 10.1109/EMBC.2018.8513086. [PubMed: 30441043]

[59]. Datta A, Truong D, Minhas P, Parra LC, Bikson M. Inter-individual variation during transcranial direct current stimulation and normalization of dose using MRI-derived computational models. Front Psychiatr 2012;3:91. 10.3389/fpsyt.2012.00091.

[60]. Wang S-MS, Huang Y-J, Chen J-JJ, Wu C-W, Chen C-A, Lin C-W, Nguyen V-T, Peng C-W. Designing and pilot testing a novel high-definition transcranial burst electrostimulation device for neurorehabilitation. J Neural Eng 2021;18:056030. 10.1088/1741-2552/ac23be.

[61]. Dallmer-Zerbe I, Popp F, Lam AP, Philipsen A, Herrmann CS. Transcranial alternating current stimulation (tACS) as a tool to modulate P300 amplitude in attention deficit hyperactivity disorder (ADHD): preliminary findings. Brain Topogr 2020;33:191–207. 10.1007/s10548-020-00752-x. [PubMed: 31974733]

[62]. Klomjai W, Siripornpanich V, Aneksan B, Vimolratana O, Permpoonputtana K, Tretriluxana J, Thichanpiang P. Effects of cathodal transcranial direct current stimulation on inhibitory and attention control in children and adolescents with attention-deficit hyperactivity disorder: a pilot randomized sham-controlled crossover study. J Psychiatr Res 2022. 10.1016/j.jpsychires.2022.02.032.

[63]. Tan SJ, Filmer HL, Dux PE. Age-related differences in the role of the prefrontal cortex in sensory-motor training gains: a tDCS study. Neuropsychologia 2021;158:107891. 10.1016/j.neuropsychologia.2021.107891. [PubMed: 34004221]

[64]. Bjekić J, Vulić K, Živanović M, Vujičić J, Ljubisavljević M, Filipović SR. The immediate and delayed effects of single tDCS session over posterior parietal cortex on face-word associative memory. Behav Brain Res 2019;366:88–95. 10.1016/j.bbr.2019.03.023. [PubMed: 30880221]

[65]. Luckey AM, McLeod SL, Mohan A, Vanneste S. Potential role for peripheral nerve stimulation on learning and long-term memory: a comparison of alternating and direct current stimulations. Brain Stimul 2022. 10.1016/j.brs.2022.03.001.

[66]. Federica C, Edwards G, Tyler S, Parrott D, Grossman E, Lorella B. Attention network modulation via tRNS correlates with attention gain. eLife 2021;10. 10.7554/eLife.63782.

[67]. Kasten FH, Wendeln T, Stecher HI, Herrmann CS. Hemisphere-specific, differential effects of lateralized, occipital–parietal α- versus γ-tACS on endogenous but not exogenous visual-spatial attention. Sci Rep 2020;10: 12270. 10.1038/s41598-020-68992-2. [PubMed: 32703961]

[68]. Luna FG, Román-Caballero R, Barttfeld P, Lupiáñez J, Martín-Arévalo E. A High-Definition tDCS and EEG study on attention and vigilance: brain stimulation mitigates the executive but not the arousal vigilance decrement. Neuropsychologia 2020;142:107447. 10.1016/j.neuropsychologia.2020.107447. [PubMed: 32243885]

[69]. Takeuchi N, Sudo T, Oouchida Y, Mori T, Izumi S-I. Synchronous neural oscillation between the right inferior fronto-parietal cortices contributes to body awareness. Front Hum Neurosci 2019;13. 10.3389/fnhum.2019.00330.

[70]. Bhattacharjee S, Kashyap R, Rapp B, Oishi K, Desmond JE, Chen SHA. Simulation analyses of tDCS montages for the investigation of dorsal and ventral pathways. Sci Rep 2019;9:12178. 10.1038/s41598-019-47654-y. [PubMed: 31434911]

[71]. Labree B, Corrie H, Karolis V, Didino D, Cappelletti M. Parietal alpha-based inhibitory abilities are causally linked to numerosity discrimination. Behav Brain Res 2020;387:112564. 10.1016/j.bbr.2020.112564. [PubMed: 32081712]

[72]. Li N, Wang Y, Jing F, Zha R, Wei Z, Yang L-Z, Geng X, Tanaka K, Zhang X. A role of the lateral prefrontal cortex in the congruency sequence effect revealed by transcranial direct current stimulation. Psychophysiology 2021;58:e13784. 10.1111/psyp.13784. [PubMed: 33559273]

[73]. Tesche CD, Houck JM. Discordant alpha-band transcranial alternating current stimulation affects cortico-cortical and cortico-cerebellar connectivity. Brain Connect 2020;10:170–82. 10.1089/brain.2019.0710. [PubMed: 32216454]

[74]. Ehrhardt SE, Filmer HL, Wards Y, Mattingley JB, Dux PE. The influence of tDCS intensity on decision-making training and transfer outcomes. J Neurophysiol 2021;125:385–97. 10.1152/jn.00423.2020. [PubMed: 33174483]

[75]. Garofalo S, Battaglia S, Starita F, di Pellegrino G. Modulation of cue-guided choices by transcranial direct current stimulation. Cortex 2021;137: 124–37. 10.1016/j.cortex.2021.01.004. [PubMed: 33609898]

[76]. Hu Y, Philippe R, Guigon V, Zhao S, Derrington E, Corgnet B, Bonaiuto JJ, Dreher J-C. In: Perturbation of right dorsolateral prefrontal cortex makes power holders less resistant to tempting bribes. Psychol Sci 09567976211042379; 2022. 10.1177/09567976211042379.

[77]. Manuel AL, Murray NWG, Piguet O. Transcranial direct current stimulation (tDCS) over vmPFC modulates interactions between reward and emotion in delay discounting. Sci Rep 2019;9:18735. 10.1038/s41598-019-55157-z. [PubMed: 31822732]

[78]. Ergo K, Loof ED, Debra G, Pastötter B, Verguts T. Failure to modulate reward prediction errors in declarative learning with theta (6 Hz) frequency transcranial alternating current stimulation. PLoS One 2020;15:e0237829. 10.1371/journal.pone.0237829. [PubMed: 33270685]

[79]. Riddle J, Alexander ML, Schiller CE, Rubinow DR, Frohlich F. Reduction in left frontal alpha oscillations by transcranial alternating current stimulation in major depressive disorder is context dependent in a randomized clinical trial. Biol Psychiatr: Cognit Neurosci Neuroimag 2021. 10.1016/j.bpsc.2021.07.001.

[80]. Gebodh N, Esmaeilpour Z, Datta A, Bikson M. Dataset of concurrent EEG, ECG, and behavior with multiple doses of transcranial electrical stimulation. Sci Data 2021;8:274. 10.1038/s41597-021-01046-y. [PubMed: 34707095]

[81]. Jones KT, Johnson EL, Tauxe ZS, Rojas DC. Modulation of auditory gamma-band responses using transcranial electrical stimulation. J Neurophysiol 2020b;123:2504–14. 10.1152/jn.00003.2020. [PubMed: 32459551]

[82]. Lazarev VV, Gebodh N, Tamborino T, Bikson M, Caparelli-Daquer EM. Experimental-design specific changes in spontaneous EEG and during intermittent photic stimulation by high definition transcranial direct current stimulation. Neuroscience 2020;426:50e8. 10.1016/j.neuroscience.2019.11.016. [PubMed: 31785357]

[83]. Popp F, Dallmer-Zerbe I, Philipsen A, Herrmann CS. Challenges of P300 modulation using transcranial alternating current stimulation (tACS). Front Psychol 2019;10. 10.3389/fpsyg.2019.00476.

[84]. Takeuchi N, Terui Y, Izumi S-I. Oscillatory entrainment of neural activity between inferior frontoparietal cortices alters imitation performance. Neuropsychologia 2021;150:107702. 10.1016/j.neuropsychologia.2020.107702. [PubMed: 33276036]

[85]. Huang Y, Mohan A, McLeod SL, Luckey AM, Hart J, Vanneste S. Polarity-specific high-definition transcranial direct current stimulation of the anterior and posterior default mode network improves remote memory retrieval. Brain Stimul 2021;14:1005–14. 10.1016/j.brs.2021.06.007. [PubMed: 34182233]

[86]. Koolschijn RS, Emir UE, Pantelides AC, Nili H, Behrens TEJ, Barron HC. The Hippocampus and neocortical inhibitory engrams protect against memory interference. Neuron 2019;101:528–41. 10.1016/j.neuron.2018.11.042.e6. [PubMed: 30581011]

[87]. Pyke W, Vostanis A, Javadi A-H. Electrical brain stimulation during a retrieval-based learning task can impair long-term memory. J Cogn Enhanc 2021;5:218–32. 10.1007/s41465-020-00200-5.

[88]. Filmer HL, Griffin A, Dux PE. For a minute there, I lost myself … dosage dependent increases in mind wandering via prefrontal tDCS. Neuropsychologia 2019b;129:379–84. 10.1016/j.neuropsychologia.2019.04.013. [PubMed: 31071322]

[89]. Filmer HL, Marcus LH, Dux PE. Stimulating task unrelated thoughts: tDCS of prefrontal and parietal cortices leads to polarity specific increases in mind wandering. Neuropsychologia 2021;151:107723. 10.1016/j.neuropsychologia.2020.107723. [PubMed: 33307101]

[90]. Ashcroft J, Patel R, Woods AJ, Darzi A, Singh H, Leff DR. Prefrontal transcranial direct-current stimulation improves early technical skills in surgery. Brain Stimul 2020;13:1834–41. 10.1016/j.brs.2020.10.013. [PubMed: 33130252]

[91]. Caesley H, Sewell I, Gogineni N, Javadi A-H. Transcranial direct current stimulation does not improve performance in a whole-body movement task. 10.1101/2021.01.25.428100; 2021.

[92]. Greeley B, Barnhoorn JS, Verwey WB, Seidler RD. Multi-session transcranial direct current stimulation over primary motor cortex facilitates sequence learning, chunking, and one year retention. Front Hum Neurosci 2020;14. 10.3389/fnhum.2020.00075.

[93]. Greeley B, Seidler RD. Differential effects of left and right prefrontal cortex anodal transcranial direct current stimulation during probabilistic sequence learning. J Neurophysiol 2019;121:1906–16. 10.1152/jn.00795.2018. [PubMed: 30917064]

[94]. King BR, Rumpf J-J, Heise K-F, Veldman MP, Peeters R, Doyon J, Classen J, Albouy G, Swinnen SP. Lateralized effects of post-learning transcranial direct current stimulation on motor memory consolidation in older adults: an fMRI investigation. Neuroimage 2020;117323. 10.1016/j.neuroimage.2020.117323. [PubMed: 32882377]

[95]. Sehatpour P, Donde C, Hoptman MJ, Kreither J, Adair D, Dias E, Vail B, Rohrig S, Silipo G, Lopez-Calderon J, Martinez A, Javitt DC. Network-level mechanisms underlying effects of transcranial direct current stimulation (tDCS) on visuomotor learning. Neuroimage 2020;117311. 10.1016/j.neuroimage.2020.117311. [PubMed: 32889116]

[96]. Boukarras S, Özkan DG, Era V, Moreau Q, Tieri G, Candidi M. Midfrontal theta tACS facilitates motor coordination in dyadic human-avatar interactions. J Cognit Neurosci 2022;1–18. 10.1162/jocn_a_01834.

[97]. Patel R, Suwa Y, Kinross J, von Roon A, Woods AJ, Darzi A, Singh H, Leff DR. Neuroenhancement of surgeons during robotic suturing. Surg Endosc 2021. 10.1007/s00464-021-08823-1.

[98]. Walia P, Fu Y, Schwaitzberg SD, Intes X, De S, Cavuoto L, Dutta A. Neuroimaging guided tES to facilitate complex laparoscopic surgical tasks - insights from functional near-infrared spectroscopy. Annu Int Conf IEEE Eng Med Biol Soc 2021:7437–40. 10.1109/EMBC46164.2021.9631005.2021. [PubMed: 34892815]

[99]. Arora Y, Dutta A. Transcranial electrical stimulation effects on neurovascular coupling (preprint). In Review, 10.21203/rs.3.rs-1429599/v1; 2022.

[100]. Frohlich F, Riddle J, Abramowitz JS. Transcranial alternating current stimulation for the treatment of obsessive-compulsive disorder? Brain Stimul: Basic, Translational, and Clinical Research in Neuromodulation 2021;14: 1048–50. 10.1016/j.brs.2021.06.014.

[101]. Damercheli S, Ramne M, Ortiz-Catalan M. Transcranial direct current stimulation (tDCS) for the treatment and investigation of phantom limb pain (PLP). Psychoradiology 2022;2:23–31. 10.1093/psyrad/kkac004.

[102]. Garcia S, Hampstead BM. HD-tDCS as a neurorehabilitation technique for a case of post-anoxic leukoencephalopathy. Neuropsychol Rehabil 2020:1–21. 10.1080/09602011.2020.1845749.0.

[103]. Reyes C, Padrón I, Nila Yagual S, Marrero H. Personality traits modulate the effect of tDCS on reading speed of social sentences. Brain Sci 2021;11:1464. 10.3390/brainsci11111464. [PubMed: 34827463]

[104]. Sreeraj VS, Suhas S, Parlikar R, Selvaraj S, Dinakaran D, Shivakumar V, Narayanaswamy JC, Venkatasubramanian G. Effect of add-on transcranial alternating current stimulation (tACS) on persistent delusions in schizophrenia. Psychiatr Res 2020;290:113106. 10.1016/j.psychres.2020.113106.

[105]. Jafari E, Alizadehgoradel J, Pourmohseni Koluri F, Nikoozadehkordmirza E, Refahi M, Taherifard M, Nejati V, Hallajian A-H, Ghanavati E, Vicario CM, Nitsche MA, Salehinejad MA. Intensified electrical stimulation targeting lateral and medial prefrontal cortices for the treatment of social anxiety disorder: a randomized, double-blind, parallel-group, dose-comparison study. Brain Stimul 2021;14:974–86. 10.1016/j.brs.2021.06.005. [PubMed: 34167918]

[106]. Bao S-C, Wong W-W, Leung TWH, Tong K-Y. Cortico-muscular coherence modulated by high-definition transcranial direct current stimulation in people with chronic stroke. IEEE Trans Neural Syst Rehabil Eng 2019;27: 304–13. 10.1109/TNSRE.2018.2890001. [PubMed: 30596581]

[107]. He Q, Yang X-Y, Gong B, Bi K, Fang F. Boosting visual perceptual learning by transcranial alternating current stimulation over the visual cortex at alpha frequency. Brain Stimul 2022. 10.1016/j.brs.2022.02.018.

[108]. Zhu M, Hardstone R, He BJ. Neural oscillations promoting perceptual stability and perceptual memory during bistable perception. Sci Rep 2022;12:2760. 10.1038/s41598-022-06570-4. [PubMed: 35177702]

[109]. Cerreta AGB, Mruczek REB, Berryhill ME. Predicting working memory training benefits from transcranial direct current stimulation using resting-state fMRI. Front Psychol 2020;11:2627. 10.3389/fpsyg.2020.570030.

[110]. Johnson EL, Arciniega H, Jones KT, Kilgore-Gomez A, Berryhill ME. Individual predictors and electrophysiological signatures of working memory enhancement in aging. Neuroimage 2022;250:118939. 10.1016/j.neuroimage.2022.118939. [PubMed: 35104647]

[111]. Jones KT, Johnson EL, Berryhill ME. Frontoparietal theta-gamma interactions track working memory enhancement with training and tDCS. Neuroimage 2020a;211:116615. 10.1016/j.neuroimage.2020.116615. [PubMed: 32044440]

[112]. Murphy OW, Hoy KE, Wong D, Bailey NW, Fitzgerald PB, Segrave RA. Transcranial random noise stimulation is more effective than transcranial direct current stimulation for enhancing working memory in healthy individuals: behavioural and electrophysiological evidence. Brain Stimul 2020;13:1370–80. 10.1016/j.brs.2020.07.001. [PubMed: 32659482]

[113]. Nikolin S, Lauf S, Loo CK, Martin D. Effects of high-definition transcranial direct current stimulation (HD-tDCS) of the intraparietal sulcus and dorsolateral prefrontal cortex on working memory and divided attention. Front Integr Neurosci 2019;12:64. 10.3389/fnint.2018.00064. [PubMed: 30670954]

[114]. Nissim NR, O'Shea A, Indahlastari A, Kraft JN, von Mering O, Aksu S, Porges E, Cohen R, Woods AJ. Effects of transcranial direct current stimulation paired with cognitive training on functional connectivity of the working memory network in older adults. Front Aging Neurosci 2019;11:340. 10.3389/fnagi.2019.00340. [PubMed: 31998111]

[115]. Thompson L, Khuc J, Saccani MS, Zokaei N, Cappelletti M. Gamma oscillations modulate working memory recall precision. Exp Brain Res 2021;239: 2711–24. 10.1007/s00221-021-06051-6. [PubMed: 34223958]

[116]. Ashburner J, Friston KJ. Unified segmentation. Neuroimage 2005;26:839–51. 10.1016/j.neuroimage.2005.02.018. [PubMed: 15955494]

[117]. Evans AC, Collins DL, Mills SR, Brown ED, Kelly RL, Peters TM. 3D statistical neuroanatomical models from 305 MRI volumes. In: Nuclear science symposium and medical imaging conference, 1993., 1993 IEEE conference record. Presented at the nuclear science symposium and medical imaging conference, 1993. 3. IEEE Conference Record.; 1993. p. 1813–7. 10.1109/NSSMIC.1993.373602.

[118]. Rush S, Driscoll DA. EEG electrode sensitivity–an application of reciprocity. IEEE Trans Biomed Eng 1969;16:15–22 [PubMed: 5775600]

[119]. Tutorials/Plugins. Brainstorm [WWW Document], n.d. URL, https://neuroimage.usc.edu/brainstorm/Tutorials/Plugins.5.12.21.

[120]. Tadel F, Baillet S, Mosher JC, Pantazis D, Leahy RM. Brainstorm: a user-friendly application for MEG/EEG analysis. Comput Intell Neurosci 2011. 10.1155/2011/879716. 2011.

[121]. Hirsch L, Huang Y, Parra LC. Segmentation of MRI head anatomy using deep volumetric networks and multiple spatial priors. JMI 2021;8:034001. 10.1117/1.JMI.8.3.034001. [PubMed: 34159222]

[122]. Jog M, Jann K, Yan L, Huang Y, Parra L, Narr K, Bikson M, Wang DJJ. Concurrent imaging of markers of current flow and neurophysiological changes during tDCS. Front Neurosci 2020;14. 10.3389/fnins.2020.00374.

[123]. Louviot S, Tyvaert L, Maillard LG, Colnat-Coulbois S, Dmochowski J, Koessler L. Transcranial Electrical Stimulation generates electric fields in deep human brain structures. Brain Stimul 2022;15:1–12. 10.1016/j.brs.2021.11.001. [PubMed: 34742994]

[124]. Eroglu HH, Puonti O, Göksu C, Gregersen F, Siebner HR, Hanson LG, Thielscher A. Human in-vivo magnetic resonance current density imaging of the brain by optimizing head tissue conductivities. Brain Stimul: Basic, Translational, and Clinical Research in Neuromodulation 2021;14:1591–2. 10.1016/j.brs.2021.10.012.

[125]. Fusco G, Fusaro M, Aglioti SM, n.d. Midfrontal-occipital q-tACS modulates cognitive conflicts related to bodily stimuli 10.

[126]. Schulreich S, Schwabe L, n.d. Causal role of the dorsolateral prefrontal cortex in belief updating under uncertainty. Cerebr Cortex. 10.1093/cercor/bhaa219.

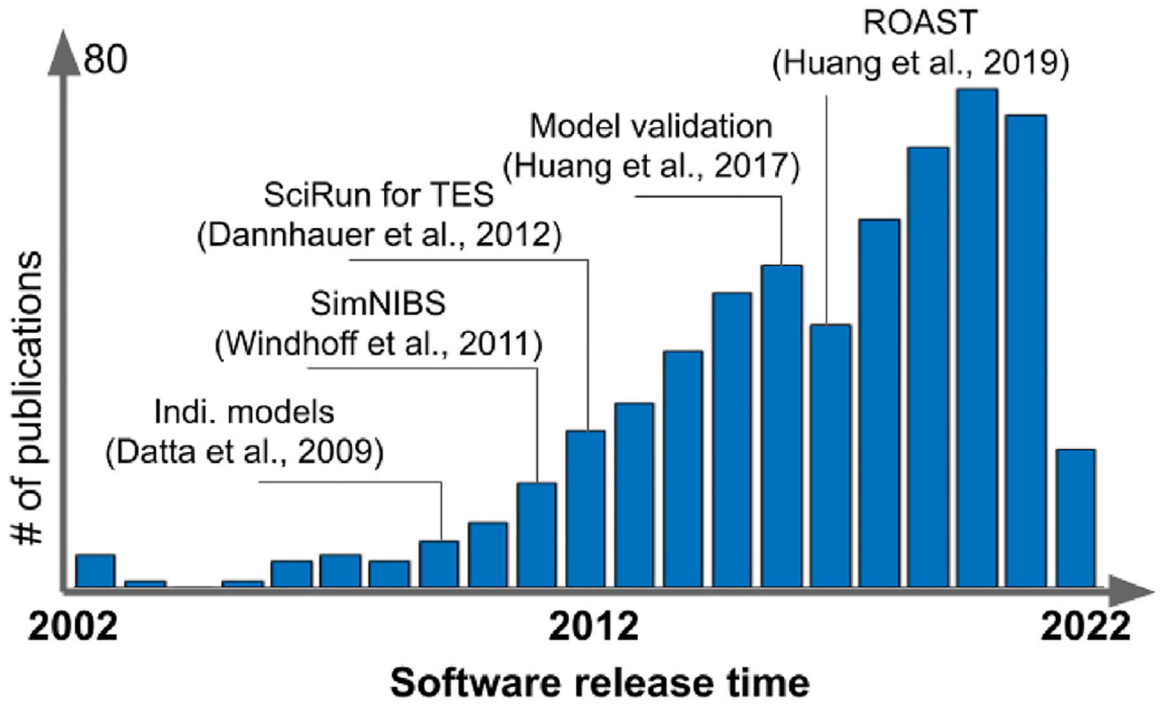

Fig. 1.

Number of publications in PubMed returned by searching “computational models transcranial electrical stimulation”. Major open-source software for TES modeling are noted at their time of release. Note the release time of the software may be earlier than the time of their corresponding publication.

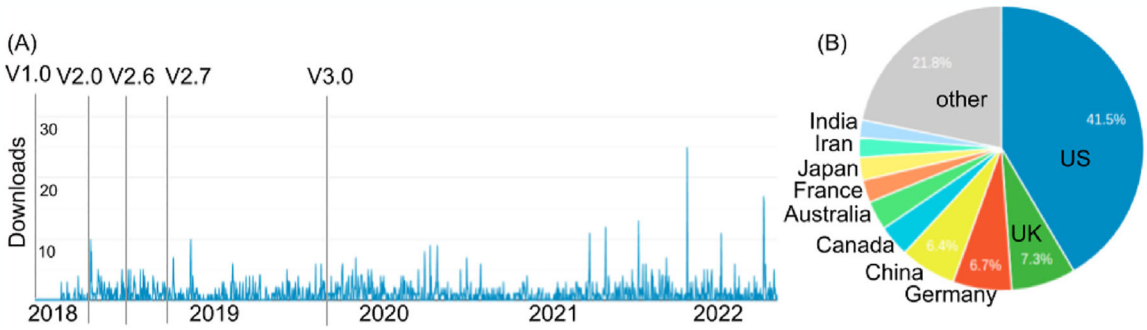

Fig. 2.

Traffic data from Google Analytics for the hosting website of ROAST. (A) Daily downloads since the first release (V1.0). Time points of major version upgrades are noted by vertical gray lines. Note that traffic data are not available immediately after V1.0 as we did not set up traffic tracking until February 2018. (B) Geographical distributions of visitors.

Table 1

Clinical studies that used ROAST to model individual heads under different research contexts.

Applications	Number of Subjects Modeled (References)	Use Purposes
Aging effects	N = 587 [22]	(I), (III)
	N = 130 [23]	(I), (II), (V)
	N = 54 [24]	(I), (II), (III)
Alzheimer/Dementia	N = 2 [25]	(II), (III)
	N = 60 [26]	(II), (III), (VI)
Brain tumor/lesion	N = 2 [27]	(I), (II)
	N = 2 [28]	(II), (VI)
	N = 8 [29]	(I), (II), (VI)
Cerebellar stimulation	N = 4 [30]	(I), (II), (VI)
	N = 12 [31]	(I), (II), (VI)
	N = 18 [32]	(I), (III), (IV)
	N = 10 [33]	(I), (III), (IV)
	N = 12 [34]	(I), (III), (IV)
	N = 25 [35]	(I), (III), (IV)
Cognition	N = 16 [36]	(I), (II), (VI)
Depression	N = 151 [37]	(I)
Epilepsy	N = 2 [38]	(I)
	N = 12 [39]	(I), (II), (VI)
Functional connectivity	N = 10 [40]	(I), (II)
Inter-individual variability	N = 57 [41]	(I), (II), (IV), (V) (VI)
	N = 50 [42]	(I), (II), (V), (VI)
	N = 14 [43]	(I), (II), (VI)
	N = 2 [44]	(I), (IV)
	N = 32 [45]	(II)
	N = 47 [46]	(I)
	N = 60 [47]	(I)
	N = 240 [48]	(I), (II), (III), (VI)
	N = 29 [49]	(I), (V)

Applications	Number of Subjects Modeled (References)	Use Purposes
	N = 47 [50]	(I), (V)
	N = 15 [51]	(II), (VI)
	N = 90 [52]	(II), (V), (VI)
Schizophrenia	N = 21 [53]	(I), (II), (VI)
	N = 17 [54]	(I)
Substance use disorder	N = 5 [55,56]	(II), (IV), (V), (VI)
Working memory and attention	N = 15 [57]	(I), (II)
Total	N = 1858	

Use purposes include: (I) ROI analysis of E-field against clinical outcomes; (II) Visualization of the E-field at ROI; (III) Voxel-based morphometry; (IV) Optimization of the stimulation; (V) Dose control; (VI) Visualization of electrode placement.

Table 2

Details in the studies reported in Table 1. Electrode names follow international 10/05 convention unless otherwise specified.

Number of Subjects Modeled (References)	Electrode montage (high-definition (H) or conventional(C))	Which brain area is specifically studied?	E-field or current density output by ROAST at studied brain area (normalized to 1 mA stimulation)	E-field correlates with the clinical outcome?	Patients or healthy subjects?
N = 587 [22]	F3-F4 & C3-Fp2 (C)	Entire brain	Average median were 0.007 A/m^2 and 0.009 A/m^2 for F3-F4, and 0.011 A/m^2 and 0.012 A/m^2 for C3-Fp2 montage in the older and young adult cohort, respectively.	E-field inversely correlated with brain atrophy	Healthy old and young adults
N = 130 [23]	F3-F4 (C)	White matter hyperintensities (WMH)	WMH regions had a maximum of 1.77 V/m.	Changes in E-field positively correlated with the total lesion volume.	Healthy old adults
N = 54 [24]	F3 (C)	Left M1 and DLPFC	N/A	E-field decreased with scalp-to-cortex distance in mild cognitive impairment converters.	Normal aging and mild cognitive impairment converters
N = 2 [25]	F3-F4 (C)	Frontal cortex	Peak E-field of 0.3 V/m.	N/A	Patients with early stage Alzheimer's disease
N = 60 [26]	FT7-AF8 (C)	Left anterior/middle temporal lobe	N/A	N/A	Patients with dementia
N = 2 [27]	Anterior-posterior and left-right array (H)	Brain tumor	Average E-field at tumor is 0.17 V/m.	Presence of peritumoral edema resulted in decreased E-field magnitude within the tumor.	Patients with brain tumor
N = 2 [28]	F3-F4, P3-P4 (C&H)	Cortical surface	Peak E-field of 0.16 V/m.	N/A	Healthy and patient with multiple sclerosis
N = 8 [29]	C3-FP1 (C)	Left M1	Average E-field is 0.12 ± 0.03 V/m (range 0.08–0.17 V/m)	E-field magnitude applied to the left M1 correlated with changes in global connectivity of the right M1.	Patients with left-sided glioma
N = 4 [30]	E133-E18 in EGI HCGSN-256 system (C); anode Iz - cathodes Oz, O2, P8, PO8 (H)	Cerebellum	0.2 V/m - 0.25 V/m under montage E133-E18; Average 0.1 V/m under montage anode Iz - cathodes Oz, O2, P8, PO8	Amplitude and orientation of E-field is related to bursting and complex spiking in Purkinje cells in the cerebellum.	Healthy subjects
N = 12 [31]	PO9h - PO10h Exx7 - Exx8 (H)	Cerebellum	Peak E-field of 0.15 V/m.	Mean E-field strength was a good predictor of the latent variables of oxy-hemoglobin (O2Hb) concentrations and log10-transformed EEG bandpower.	Patients with hemiparetic chronic stroke
N = 18 [32]	Celnik montage (C)	Cerebellum	Peak E-field of 0.15 V/m.	E-Field increased significantly at the targeted cerebellar hemisphere at an old age.	Healthy subjects
N = 10 [33]	PO9h-PO10h Exx7-Exx8 (H)	Cerebellum	Average ~0.04 V/m.	A linear relationship between successful functional reach in post-stroke balance rehabilitation and E-field strength was found.	Patients with chronic stroke

Number of Subjects Modeled (References)	Electrode montage (high-definition (H) or conventional(C))	Which brain area is specifically studied?	E-field or current density output by ROAST at studied brain area (normalized to 1 mA stimulation)	E-field correlates with the clinical outcome?	Patients or healthy subjects?
N = 12 [34]	PO9h-PO10h Exx7-Exx8 (H)	Cerebellum	Average ~0.05 V/m.	The changes in the quantitative gait parameters were found to be correlated to the mean E-field strength in the cerebellar lobules.	Patients with chronic stroke
N = 25 [35]	I1-Exx25 (C)	Cerebellum	N/A	tDCS-related metabolite changes may be related to the strength of the E-field induced at the region of interest.	Healthy subjects
N = 16 [36]	CP5-CZ TP7-TP8 (C)	Lexical (ventral) and sublexical (dorsal) pathways for language	Average ~0.04 A/m^2.	Sub-lexical proficiency is associated with greater effects of tDCS stimulation.	Healthy subjects
N = 151 [37]	C2-FT8 (H)	Left amygdala and left hippocampus	Average ~0.11 V/m.	High electrical fields are strongly associated with robust volume changes in a dose-dependent fashion.	Patients with depression
N = 2 [38]	Left and right earlobes and infra-auricular (H)	Deep brain sampled by sEEG electrodes	Maximum of 0.4 V/m.	E-fields measured in vivo are highly correlated with the predicted ones.	Patients with epilepsy
N = 12 [39]	Various montages such as T8, Oz - T7 (H)	Deep brain sampled by sEEG electrodes	Maximum of 0.5 V/m.	E-fields measured in vivo are highly correlated with the predicted ones.	Patients with epilepsy
N = 10 [40]	PO7, PO3 - Cz (H)	Motion area	Average E-field magnitude on the left motion area is 0.16 V/m, and on the right motion area 0.09 V/m.	Functional connectivity (between motion area and any other region of interest) increases in proportion to the E-field strength in the region of interest.	Healthy subjects
N = 57 [41]	Cz-Oz (C)	Entire brain	Average E-field is 0.13 ± 0.05 V/m (min = 0.08 V/m, max = 0.36 V/m).	Variability of power increase in alpha-oscillations was significantly predicted by E-field from individual modeling.	Healthy subjects
N = 50 [42]	Directional montage: CP5-FC1 (H); Conventional montage: C3-FP2 (H)	Left M1	Directional montage: 0.19 ± 0.04 V/m; Conventional montage: 0.18 ± 0.04 V/m.	Fixed-dose tDCS yields substantially variable E-field intensities in left M1 due to inter-individual variability.	Healthy subjects
N = 14 [43]	F3-F4 (C)	Entire brain	N/A	Median E-field in brain regions near the electrodes were positively related to tDCS intervention responses.	Healthy older adults
N = 2 [44]	Fp2-CCP3 (H) Exx20-FFT7h or F7h (H)	M1 Broca's area (BA44)	Fp2-CCP3: 0.16 V/m.	Lesions that were larger, closer to the ROI, and had a higher conductance tended to have the greatest impact on E-field magnitude.	Healthy subjects, with lesions added in the model
N = 32 [45]	AF3-CP5 (C)	Entire brain	N/A	N/A	Healthy subjects
N = 47 [46]	F3-F4 (C)	Inferior frontal gyrus	Median of 0.047 V/m.	Including E-field in the regressions did not change the effect of tDCS.	Healthy subjects
N = 60 [47]	F3-F4 (H)	Frontal cortex	0.06–0.10 V/m.	E-field accounted for 54%−65% of the variance in tACS-related performance improvements.	Healthy old adults
N = 240 [48]	CP5-CZ (C)	Inferior parietal lobule (IPL)	Average ~0.2 mA/m^2.	Across all age groups, CSF and gray matter volumes significantly predicted the E-field at the target sites.	Healthy subjects

Number of Subjects Modeled (References)	Electrode montage (high-definition (H) or conventional(C))	Which brain area is specifically studied?	E-field or current density output by ROAST at studied brain area (normalized to 1 mA stimulation)	E-field correlates with the clinical outcome?	Patients or healthy subjects?
	F3-FP2 (C)	Middle frontal gyrus (MFG)			
N = 29 [49]	Left motor hotspot and left neck (C)	Motor cortex	Average 0.17 V/m.	Transcranial electrical stimulation motor threshold significantly correlated with the ROI-based reverse-calculated tDCS dose determined by E-field modeling.	Healthy subjects
N = 47 [50]	1 cm posterior to F3-F4 (C)	Left prefrontal cortex	N/A	Cortical thickness in left prefrontal cortex correlates with anodal tDCS efficacy.	Healthy subjects
N = 15 [51]	CP5-Cz (C)	Entire brain	Average ~0.14 mA/m^2	N/A	Healthy subjects
N = 90 [52]	F3 and the right supraorbital (C)	Left middle frontal gyrus	Average ~0.12 mA/m^2	N/A	Healthy subjects
N = 21 [53]	Anode: left DLPFC (between F3 & FP1 Cathode: left TPOJ (between T3 & P3) (C)	TPOJ and auditory association regions	Average ~0.25 V/m.	E-field strength at anterior regions correlated significantly with less robust clinical response.	Patients with schizophrenia
N = 17 [54]	Anode: left DLPFC (between F3 & FP1 Cathode: left TPOJ (between T3 & P3) (C)	Left transverse temporal gyrus	N/A	tDCS responders displayed higher E-field strength in the left transverse temporal gyrus at baseline compared to nonresponders.	Patients with schizophrenia
N = 5 [55,56]	OI2-E145 in EGI HCGSN-256 system (H)	Cerebellum	Average ~0.12 V/m.	N/A	Patients with stroke
N = 15 [57]	F3-F4 (C)	Left DLPFC and left VLPFC	Average median at left DLPFC was 0.0407 A/m^2, and at left VLPFC was 0.0265 A/m^2.	E-field in the left DLPFC under active stimulation positively correlated with the beta values as measured functional connectivity metrics.	Healthy old adults
N = 1858					

N/A: data not reported in the paper. EEG: electroencephalography; CSF: cerebrospinal fluid; tDCS/tACS: transcranial direct/alternating current stimulation; ROI: region of interest; DLPFC/VLPFC: dorso/ventral lateral prefrontal cortex; M1: primary motor cortex; TPOJ: temporo-parietal-occipital junction.